

Random close packing of polydisperse hard spheres

Michiel Hermes and Marjolein Dijkstra

*Soft Condensed Matter group, Debye Institute for Nanomaterials Science,
Utrecht University, Princetonplein 5, 3584 CC Utrecht, The Netherlands*

We study jammed configurations of hard spheres as a function of compression speed using an event-driven molecular dynamics algorithm. We find that during the compression, the pressure follows closely the metastable liquid branch until the system gets arrested into a glass state as the relaxation time exceeds the compression speed. Further compression yields a jammed configuration that can be regarded as the infinite pressure configuration of that glass state. Consequently, we find that the density of jammed packings varies from 0.638 to 0.658 for polydisperse hard spheres and from 0.635 to 0.645 for pure hard spheres upon decreasing the compression rate. This demonstrates that the density at which the systems falls out of equilibrium determines the density at which the system jams at infinite pressure. In addition, we give accurate data for the jamming density as a function of compression rate and size polydispersity.

PACS numbers: 82.70.Dd, 61.43.Fs, 64.70.Q-

Dense packings of hard particles are relevant for many applications ranging from the processing of granular materials to the development of new materials. In addition, hard spheres have provided a good starting point in the study of liquids, glasses, crystals, colloids, and powders. The study of dense packings of hard spheres has a long history, dating back to Kepler for crystalline packings and Bernal [1] for random packings. In 2005, Hales proved Kepler's conjecture [2] that the densest packing of identical hard spheres is achieved by the stacking of close-packed hexagonal planes yielding a packing fraction $\phi = \pi\sigma^3 N/6V \approx 0.74$. However, when a system of hard spheres is compressed quickly it does not reach this maximum density and it jams at lower densities. Jamming phenomena are generic since atomic, colloidal and granular systems can all be jammed in a state far out of equilibrium by quickly cooling, compressing or unloading [3].

Many authors speculate that the packing fraction of the densest amorphous hard-sphere configuration is well-defined [4, 5] although its precise value is not known as random-close-packing densities ϕ_{rcp} ranging from 0.634 [5] to 0.648 [6] are reported. On the other hand, Torquato *et al* [7] argued that ϕ_{rcp} is ill-defined as the density can always be increased by introducing crystalline order into the system. Very recently, it is speculated and/or deduced from mean-field models that jammed configurations can be regarded as the infinite pressure limit of glassy states [8, 9]. The reason is that the glass phase for each density on the metastable fluid branch consists of a certain group of glassy states, which will all follow the same metastable glass branch up to the same jamming density by fast compression [8, 9].

In this letter, we study jammed configurations of hard spheres as a function of compression speed. We show that denser amorphous packings can be generated even without introducing any crystalline order by lowering the compression speed. However, in the case of iden-

tical spheres, the system (partially) crystallizes for sufficiently slow compressions. Crystallization can be avoided by introducing size polydispersity. A small size polydispersity affects ϕ_{rcp} only slightly but hampers crystal growth severely. This allows us to study jamming for a wider range of compression rates. We find volume fractions ranging from 0.638 till 0.658 for hard spheres with 10% size polydispersity upon decreasing the compression rates. Additionally, we give accurate data for the jamming density ϕ_J as a function of compression rate and size polydispersity, which is important for experiments on colloidal systems. The packing fraction of a polydisperse colloidal system is often determined by setting the packing fraction of a centrifuged sediment [10] equal to the ϕ_{rcp} obtained from simulations [11, 12]. However, these simulation results are very inaccurate and do not take into account any compression rate dependence, casting doubts on the accuracy of the volume fractions determined in experiments via this route. As our results show that the jamming density strongly depends on the compression rate, we prefer to denote the density of the jammed configuration with the jamming density ϕ_J rather than with the random-close-packing density ϕ_{rcp} .

We perform simulations with the event driven molecular dynamics algorithm of Ref. [13]. Modifications as described by Speedy [6] were used to fix the temperature of the system and to define a compression speed $\Gamma = d\sigma/dt$, where we use the MD time as our unit of time. In addition the algorithm was adapted to keep the polydispersity constant during the particle growth [14]. The polydispersity was sampled from a log-normal distribution. The log-normal distribution is nearly identical to a normal (Gaussian) distribution for small polydispersities but has the advantage that it is zero for negative diameters.

We determine the equation of state (EOS) from simulations of 2000 particles with a size polydispersity of 10%. We average our results over 50 different runs. To check

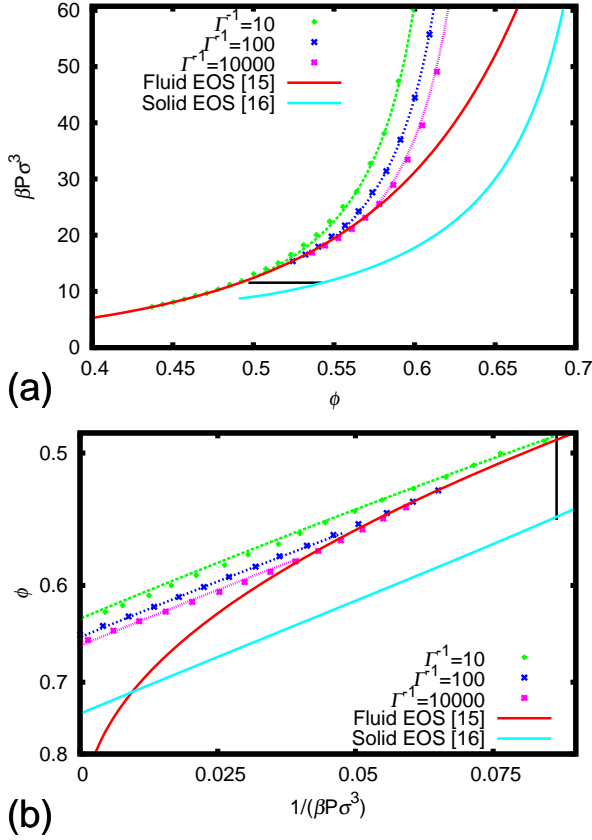


FIG. 1: a) Pressure $\beta P \sigma^3$ as a function of packing fraction ϕ for a system of hard spheres with 10% size polydispersity and for varying compression rates Γ as labeled. The red and blue (dark and light full) line denote the equilibrium equation of state for the fluid and solid phase, respectively, while the horizontal line denote fluid-solid coexistence. The dotted lines denote the fits to the simulation data using Eq. (1). b) The same results as in a) but now plotted as a function of ϕ and the inverse pressure $1/(\beta P \sigma^3)$ so that the infinite pressure limit is clearly visible.

for finite size effects we perform simulations with up to 200000 particles and we find good agreement within the statistical accuracy. We plot the EOS for varying compression rates in Fig. 1a along with the equilibrium EOS for the fluid [15] and the solid phase [16]. We checked for crystallization during our simulations, but we did not find any crystalline order in any of our compression runs. We observe that the pressure follows initially the equilibrium EOS of the fluid phase until the system becomes arrested into a glass state as the relaxation time of the system exceeds the compression rate. At this density, the pressure increases much faster than that of the equilibrium fluid EOS upon further compression. We find that the density of the jammed configuration at infinite pressure increases with slower compressions. The reason is that the system has more time to equilibrate for slow compressions, and hence the system falls out of equilibrium at a higher den-

sity on the metastable fluid branch. Further compression of this glass phase yields a jammed configuration with a density that is higher than for fast compressions. We find clear evidence that the jamming density of the amorphous packing depends strongly on the glass transition density, i.e., the density where the system becomes arrested. Therefore we find a finite range of densities for the jamming density depending on the compression procedure and history of the sample.

This behaviour is well known for molecular glasses [17]. Indeed, Fig. 1a resembles the picture that is found for molecular glasses with ϕ and the inverse of $\beta P \sigma^3$ playing the role of the inverse of the specific volume and the temperature, respectively. To this end, we plot our results in Fig. 1b in the $\phi - 1/(\beta P \sigma^3)$ representation, where $\beta = 1/k_B T$ with k_B Boltzmann's constant. We now find striking similarities with the sketched phase diagrams in Refs. [8, 9]. Recent theoretical calculation using the replica method by Parisi and Zamponi predict indeed that different glasses can jam at different densities upon compression, and that the pressure of the glass phase close to jamming is well-described by a power law $\beta P / \rho \propto 1/(\phi_J - \phi)$ with ϕ_J the jamming density at infinite pressure [8]. We observe in Fig. 1b an almost linear behavior for the inverse pressure as a function of ϕ for the glass phase, which we can fit remarkably well over the full range using the free volume scaling [4]:

$$\beta P \sigma^3 = a \frac{\phi_J^{1/3} \phi^{2/3}}{(\phi_J / \phi)^{1/3} - 1}, \quad (1)$$

where a and ϕ_J are fitting parameters. The leading order term of Eq. (1) yields the power law as predicted in [8], close to jamming. In addition, the theory predicts an ideal glass transition at a Kauzmann packing fraction $\phi_K = 0.617$ on the metastable fluid branch, yielding a jammed configuration upon compression of this ideal glass with a random close packing density of $\phi_{rcp} = 0.683$ [8]. However, the existence of a thermodynamic ideal glass transition is still heavily debated. We note that our results do not depend on the existence or non-existence of such a glass transition. Our results show a nonequilibrium glass transition at densities in the volume fraction range of 0.50-0.59, which is far below the theoretical predictions for the ideal glass. This is to be expected as the structural relaxation time diverges on approaching the ideal glass transition [18]. Hence, it is impossible to reach ϕ_K , since already at lower densities, the fluid gets arrested in a nonequilibrium glass as the relaxation time becomes longer than the simulation time.

In order to investigate the divergence of the structural relaxation time on approaching ϕ_K , and to estimate what the maximum density is at which we can still equilibrate a state on the metastable fluid branch, we perform constant volume simulations of a system of 20000 spheres with a 10% size polydispersity and varying packing frac-

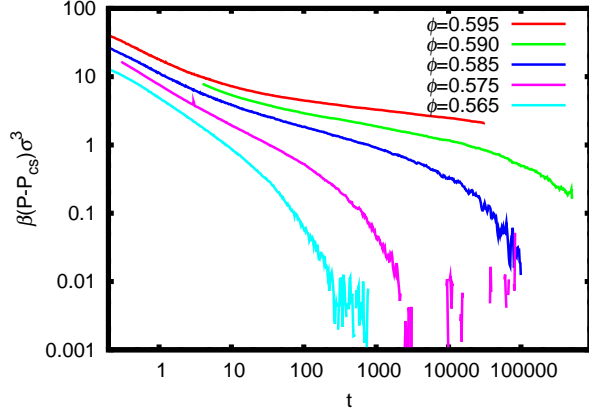


FIG. 2: The pressure difference $\beta(P - P_{CS})\sigma^3$ with respect to the Carnahan-Starling equation of state P_{CS} obtained from constant volume simulations as a function of MD time for a system of hard spheres with 10 % size polydispersity. The runs are started with an initial configuration obtained from a fast compression.

tions. We start the runs with an initial configuration obtained from a fast compression. Fig. 2 shows the pressure difference with respect to the Carnahan-Starling EOS as a function of time. We clearly see that the pressure initially decays towards an intermediate state for all ϕ . Subsequently, large collective rearrangements are required to relax the system further. Finally, we observe that the pressure reaches the value predicted by the equilibrium Carnahan-Starling EOS. The time scale for the system to equilibrate to the equilibrium fluid phase is comparable to the relaxation time τ_α that can be determined from the decay of the intermediate scattering function [18]. We clearly observe in Fig. 2 that the relaxation time diverges with packing fraction. The equilibration time of a system with 20000 particles at $\phi = 0.585$, costed more than 10^5 MD time steps, which is equivalent to two weeks on a desktop PC. The equilibration time for $\phi = 0.59$ is expected to be more than 20 weeks. Hence, the ideal glass transition at ϕ_K , and the corresponding random close packing that can be achieved by compressing the ideal glass, are both inaccessible. Instead the system will fall out of equilibrium into a non-equilibrium glass state at a density that depends strongly on the compression.

We therefor study systematically the jamming density as a function of compression speed for several size polydispersities δ . We perform simulations of 2000 particles using varying compression rates and we terminate the simulations when the time between successive collisions becomes of the same order of magnitude as our numerical accuracy, yielding pressures $\beta P\sigma^3$ up to 100000 for slow compressions. To determine the jamming density ϕ_J , we fit the equation of state close to jamming (the last few volume percent) with Eq. (1). We average our results over 50 different runs. Fig. 3a shows the jamming

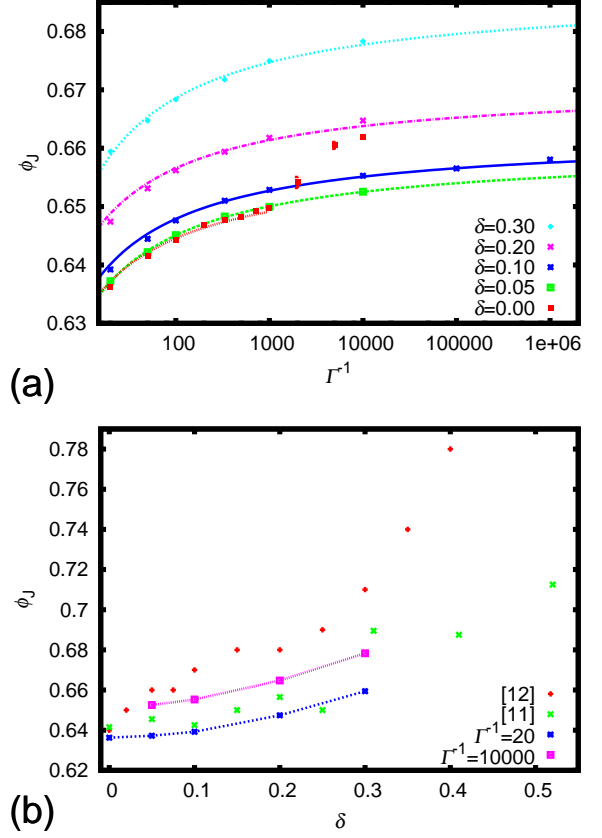


FIG. 3: a) Jamming density ϕ_J as a function of the inverse compression rate Γ^{-1} for polydispersities δ as reported in the labels. The lines denote fits to our results (see text). For monodisperse hard spheres, the line ends where (partial) crystallization is observed. b) Jamming density ϕ_J for $\Gamma^{-1} = 20$ and 10^4 as a function of size polydispersity δ . The data from Nolan *et al.* [11] and Schaertl *et al.* [12] are denoted by the crosses and plusses, respectively.

density as a function of the inverse compression rate for varying polydispersities δ . We have fitted these extrapolations with $\phi = a + b/\log(\Gamma)$, where a and b are fitting parameters. The jamming density ϕ_J for pure hard spheres ranges from 0.635 – 0.645 for $10 \leq \Gamma^{-1} \leq 1000$. For faster compressions $\Gamma^{-1} < 10$, the simulations do not yield jammed configurations and the system (partially) crystallizes for $\Gamma^{-1} > 1000$ as can be observed in Fig. 3 as ϕ_J increases rapidly. We also observe that the jamming density ϕ_J increases with increasing size polydispersity. For $\delta = 10\%$, we find that ϕ_J varies from 0.638 – 0.658. As the size polydispersity prevents crystallization, we are now able to study ϕ_J for compression rates across five orders of magnitude. Although the slope of the curves decreases with increasing Γ^{-1} (slower compressions), it is hard to justify an extrapolation to infinitely slow compression rates. Figure 3b shows the jamming density as a function of size polydispersity δ for a compression rate $\Gamma^{-1} = 20$ and 10^4 . For comparison, we also plot the data

from Nolan [11] and Schaertl [12]. Our results are close to those of Nolan [11]. The results from Schaertl *et al.* deviate from our results but can be explained since they have done single runs with low accuracy [12]. The strong dependence of the jamming density on the compression speed explains the range of densities that has been found in the literature, obtained by different authors and by using different algorithms. Our results also show that a size polydispersity of up to 5% does not increase the jamming density significantly from the monodisperse case. A much larger dependence on the polydispersity is often used in the experiments [10] based on the results of Ref. [12], casting doubts on the precise values for the volume fractions determined in experiments via this route.

In conclusion, we have studied the jamming density of hard spheres as a function of compression speed. We find that during the compression, the pressure follows closely the metastable liquid branch until the system gets arrested into a glass state. Further compression of the glass phase yields an almost linear behavior for the inverse pressure as predicted theoretically [4, 8], providing evidence that the jammed configuration can be regarded as the infinite pressure configuration of that glass state. We find, as expected, higher jamming densities for slower compression. The reason for this is that the system has more time to equilibrate for slower compressions, and hence the density increases at which the system falls out of equilibrium. Consequently, we find that the density of jammed packings varies from 0.635 to 0.645 for pure hard spheres upon decreasing the compression rate. For slower compressions we observe partial crystallization and for faster compression our simulations do not result in jammed states. For slightly polydisperse (10%) hard spheres, the jamming density varies from 0.638 to 0.658. Additionally, we give accurate data for the jamming density as a function of compression rate and size polydispersity. Our results provide evidence that there

is a fundamental difference between the ideal glass transition [8], which takes place at a fixed density (if it does exist at all), and the jamming transition [19], that takes place at a range of densities, as was already speculated by [8, 9]. However, there is a link between the density at which the system falls out of equilibrium and the density at which the system jams at infinite pressure.

-
- [1] J. Bernal and J. Mason, *Nature* **188**, 910 (1960).
 - [2] T. Hales, *Annals of mathematics* **162**, 1065 (2005).
 - [3] A. Liu and S. Nagel, *Nature* **396**, 21 (1998).
 - [4] R.D. Kamien and A.J. Liu, *Phys. Rev. Lett.* **99**, 155501 (2007).
 - [5] C. Song *et al.*, *Nature* **453**, 629 (2008).
 - [6] R.J. Speedy, *J. Chem. Phys.* **100**, 6684 (1994).
 - [7] S. Torquato *et al.*, *Phys. Rev. Lett.* **84**, 2064 (2000).
 - [8] G. Parisi and F. Zamponi, arXiv:0802.2180; *J. Chem. Phys.* **123**, 144501 (2005).
 - [9] R. Mari *et al.*, arXiv:0806.3665
 - [10] P. Ballesta *et al.*, *Phys. Rev. Lett.* **101**, 258301 (2008); R.P.A. Dullens *et al.*, *Phys. Rev. Lett.* **97**, 228301 (2006); G. Petekidis *et al.*, *Phys. Rev. E* **66**, 51402 (2002); W. Kegel and A. van Blaaderen, *Science* **287**, 290 (2000).
 - [11] G. Nolan and P. Kavanagh, *Powder technology* **72**, 149 (1992).
 - [12] W. Schaertl and H. Sillescu, *J. Stat. Phys.* **77**, 1007 (1994).
 - [13] B.D. Lubachevsky and F.H. Stillinger, *J. Stat. Phys.* **60**, 561 (1990).
 - [14] A. Kansal *et al.*, *J. Chem. Phys.* **117**, 8212 (2002).
 - [15] N.F. Carnahan and K.E. Starling, *J. Chem. Phys.* **51**, 635 (1969).
 - [16] R.J. Speedy, *J. Phys. Cond. Mat.* **10** 4387 (1998).
 - [17] W. Kauzmann, *Chem. Rev.* **43**, 219 (1948).
 - [18] G. Brambilla *et al.*, *Phys. Rev. Lett.* **102**, 085703 (2009).
 - [19] C. S. O'Hern *et al.*, *Phys. Rev. Lett.* **88**, 075507 (2002).